Report

Subcortical Connections to Human Amygdala and Changes following Destruction of the Visual Cortex

Marco Tamietto,[1,5,*] Pim Pullens,[2,5] Beatrice de Gelder,[1,2] Lawrence Weiskrantz,[3] and Rainer Goebel[2,4]

[1]Cognitive and Affective Neuroscience Laboratory, Tilburg University, 5000 LE Tilburg, The Netherlands
[2]Department of Cognitive Neuroscience, Faculty of Psychology and Neuroscience, Maastricht University, 6200 MD Maastricht, The Netherlands
[3]Department of Experimental Psychology, University of Oxford, Oxford OX1 3UD, UK
[4]Netherlands Institute for Neuroscience (NIN), an Institute of the Royal Netherlands Academy of Arts and Sciences (KNAW), 1105 BA Amsterdam, The Netherlands

Summary

Nonconscious [1–6], rapid [7, 8], or coarse [9] visual processing of emotional stimuli induces functional activity in a subcortical pathway to the amygdala involving the superior colliculus and pulvinar. Despite evidence in lower mammals [10, 11] and nonhuman primates [12], it remains speculative whether anatomical connections between these structures exist in the human brain [13–15]. It is also unknown whether destruction of the visual cortex, which provides a major input to the amygdala, induces modifications in anatomical connections along this subcortical pathway. We used diffusion tensor imaging to investigate in vivo anatomical connections between human amygdala and subcortical visual structures in ten age-matched controls and in one patient with early unilateral destruction of the visual cortex. We found fiber connections between pulvinar and amygdala and also between superior colliculus and amygdala via the pulvinar in the controls as well as in the patient. Destruction of the visual cortex led to qualitative and quantitative modifications along the pathways connecting these three structures and the changes were confined to the patient's damaged hemisphere. The present findings thus show extensive neural plasticity in the anatomical connections between subcortical visual structures of old evolutionary origin involved in the processing of emotional stimuli.

Results

We investigated whether an anatomical pathway to the amygdala (AMG), involving the superior colliculus (SC), and the visual pulvinar (Pulv), can be reconstructed in humans. This study provided an opportunity to address the controversial question as to whether functional activity previously reported along this subcortical pathway during nonconscious perception of emotional stimuli is also supported by anatomical connections among the implicated regions [14, 15]. In addition, we investigated whether the ability to process unseen emotional stimuli, often persisting in patients with damage

to the primary visual cortex (V1), may reflect compensatory mechanisms enhancing subcortical and V1-independent connections to the AMG.

We first reconstructed the fiber tracts connecting the ipsilateral SC and Pulv in each hemisphere separately and we followed their possible continuation to/from other cortical and subcortical areas. Then, we investigated with the same procedure the fibers connecting the Pulv and AMG. Finally, we traced fiber tracts supposed to selectively connect these three structures together, thereby forming a direct SC-Pulv-AMG pathway akin to the disynaptic pathway recently reported in nonhuman primates [12].

Fiber tracts reconstructed in the brain of neurologically intact subjects were compared with those found in patient G.Y. with unilateral destruction of his left V1 suffered at the age of 7 years, as the result of a traumatic brain injury. This offered the unique opportunity to study possible changes in anatomical connectivity following early loss of V1 in a patient whose residual visual ability to process emotions nonconsciously has been carefully documented and related to functional activity in the SC-Pulv-AMG pathway [2, 5, 16]. Fiber extensions to/from areas not targeted a priori were retained for further comparison with those found in either hemisphere of G.Y. only if these fiber tracts could be reconstructed in at least six of the ten control subjects.

SC-Pulv Pathway
Controls
In controls, the fiber bundles connecting the SC and Pulv were highly symmetrical in the two hemispheres and extended to/from a number of other cortical and subcortical areas, principally within the same hemisphere (Figure 1A). Fibers passing through the left SC and Pulv continued ipsilaterally to/from striate (V1) and extrastriate visual areas (V2/3, V4, MT/V5), temporal pole, posterior parietal cortex, primary motor cortex, frontal eye fields, dorsal prefrontal cortex, and orbitofrontal cortex. Subcortically, other fiber bundles were traced to/from the ipsilateral AMG, caudate, and brainstem, including periaqueductal gray. A subset of fibers crossed the midline at the level of the intercollicular commissure and continued to the contralateral (right) SC and Pulv. Fibers connecting the right SC and Pulv showed exactly the same cortical and subcortical projections reconstructed in the left hemisphere (LH). Note that all reconstructed tracts have been previously described in histological studies on nonhuman primates or in vivo diffusion tensor imaging (DTI) investigations in human subjects (see Table S4 available online). This illustrates the reliability of our tractography method and the high consistency with existing axonal connections.

A normalized measure of fiber density has been recently introduced by Yo and colleagues [17] and considered to be a reliable indicator of connection strength between two neural structures. In fact, this measure takes into account the anatomical differences between regions and subjects by weighting the number of reconstructed fibers found to connect two or more areas for the size of these structures and for the overall number of fibers passing through these regions when considered individually. We therefore quantified fiber density

[5]These authors contributed equally to the work.
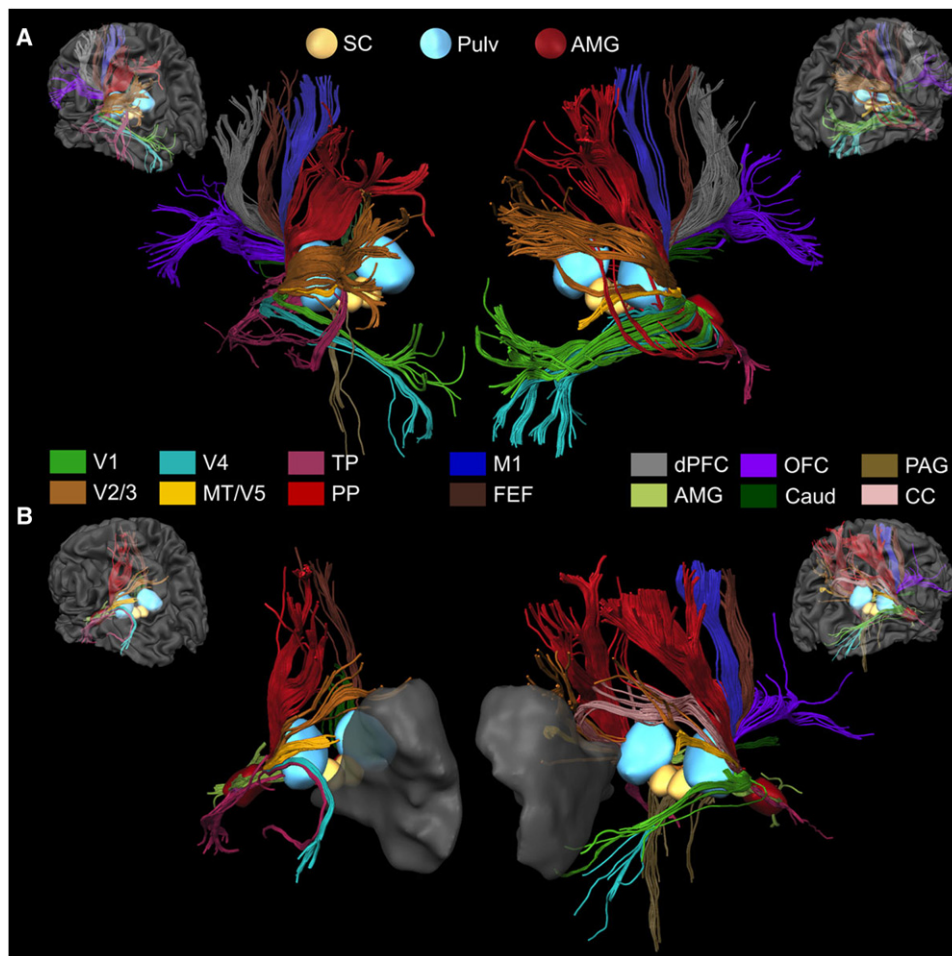*Correspondence: m.tamietto@uvt.nl

Figure 1. Reconstructed Fiber Tracts Connecting the SC with the Pulv

(A) Fiber tracts connecting the SC (yellow) with the Pulv (azure) and their continuations to other cortical and subcortical areas displayed separately for the LH and RH (left and right panel, respectively) of one representative age-matched control subject (see also Figure S2 and Table S2).

(B) The same fiber tracts reconstructed in patient G.Y. Fiber tracts extending to different cortical and subcortical areas are coded in different colors. The AMG is visible (red) as well as the lesion to left V1 in G.Y. (transparent gray).

Abbreviations: Caud, caudate; CC, corpus callosum; dPFC, dorsal prefrontal cortex; FEF, frontal eye fields; M1, primary motor cortex; OFC, orbitofrontal cortex; PAG, periacqueductal gray; PP, posterior parietal cortex; TP, temporal pole.

between ipsilateral SC and Pulv by normalizing the absolute quantity of connecting fibers for the size and fiber density of these two structures in each hemisphere and subject individually. Statistical comparisons revealed no significant difference between SC-Pulv connection strength in the LH (mean connection strength = 0.64 ± 0.12 SEM) and right hemisphere (RH) (0.75 ± 0.08) [paired sample t test: t(9) = 0.91, p = 0.39] (Figure S4).

Patient G.Y.

In the (intact) RH of G.Y., the fibers connecting the SC and Pulv extended to/from the same ipsilateral cortical and subcortical areas also identified in age-matched controls but failed to connect with the dorsal prefrontal cortex (Figure 1B). In addition, G.Y. showed prominent bilateral tracts that crossed the intercollicular commissure as well as the corpus callosum and continued to the left extrastriate areas (V2/3 and MT/V5), temporal pole, posterior parietal cortex, SC, and Pulv. In the (damaged) LH, fibers passing through the SC and Pulv projected ipsilaterally to the extrastriate visual areas (V2/3, V4, and MT/V5), temporal pole, posterior parietal cortex, and

AMG, therefore failing to connect with anterior areas in the frontal and prefrontal cortex identified in controls. Contralateral connections reached the right SC, Pulv, caudate, and frontal eye fields passing through the intercollicular commissure. In G.Y., the connection strength between left SC and Pulv (0.298) was reduced to the 36% of the connection between the same structures in his (intact) RH (0.83) and to the 46% of the mean connection strength in the LH of controls. Statistical comparison of connection strength in the right SC-Pulv pathways between G.Y. and controls showed no significant difference [one sample t test: t(9) = 1.12, p = 0.3], whereas the same comparison in the (damaged) LH revealed a significant effect [t(9) = 2.93, p = 0.02].

Pulv-AMG Pathway

Controls

Reconstructed fibers connecting the left Pulv and AMG in the controls extended to/from the ipsilateral temporal pole, dorsal prefrontal cortex, orbitofrontal cortex, caudate, and SC (Figure 2A). Fibers connecting the right Pulv and AMG continued
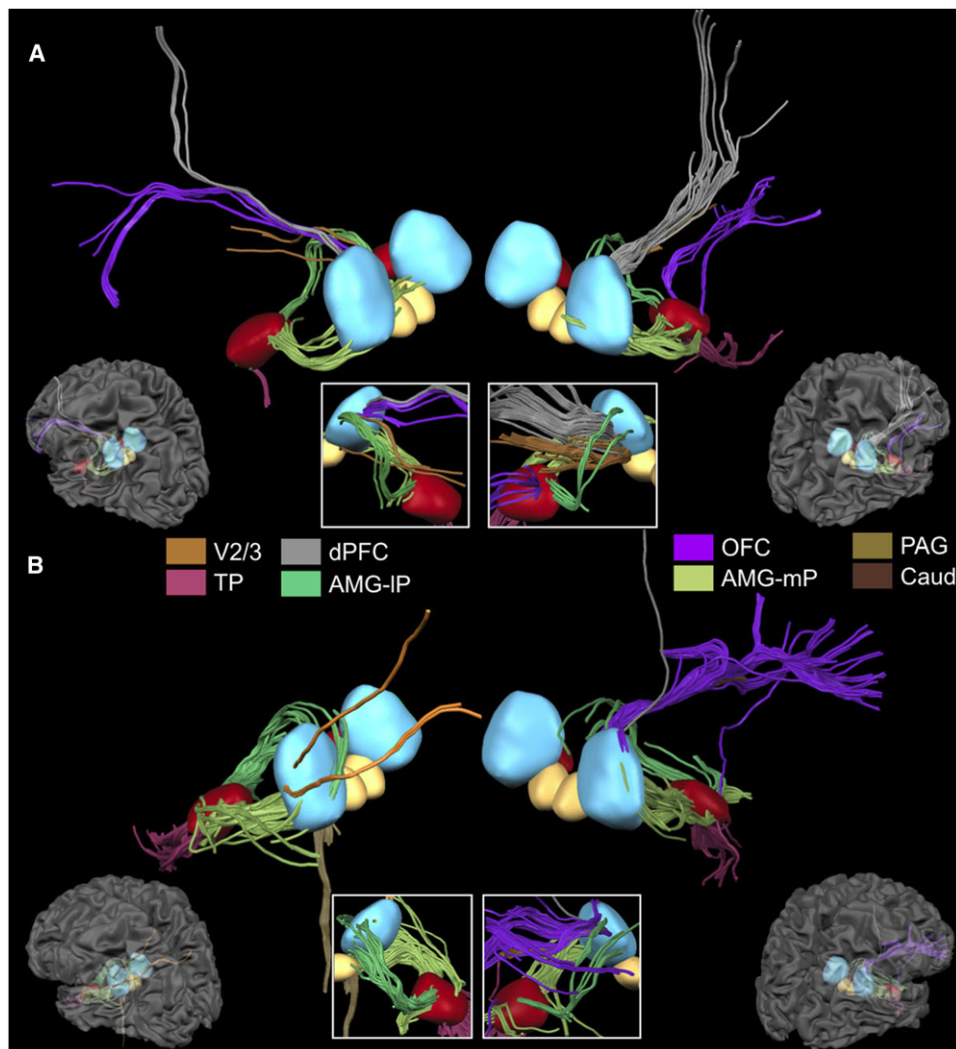
Figure 2. Reconstructed Fiber Tracts Connecting the Pulv with the AMG

(A) Fiber tracts connecting the Pulv (azure) with the AMG (red) and their continuation to other cortical and subcortical areas displayed separately for the LH and RH of one representative age-matched control subject (see also Figure S3 and Table S3).

(B) The same fiber tracts reconstructed in patient G.Y. Fiber tracts extending to different cortical and subcortical areas are coded in different colors. The SC is also visible (yellow). The white boxes display the same fibers seen in the main figure but from the opposite perspective (i.e., anteromedial view instead of posterolateral view) and limited to the space between the Pulv and AMG. Abbreviations: AMG-IP, fiber tracts connecting the AMG with inferolateral portions of the Pulv; AMG-mP, fiber tracts connecting the AMG with dorsomedial portions of the Pulv.

to/from the same areas in the RH. Noteworthy, the AMG appears to be connected with two different subregions of the ipsilateral Pulv, the dorsomedial and the inferolateral portions. This anatomical segregation is in keeping with tracer studies in nonhuman primates, indicating two efferent connections from the Pulv to the AMG that parallel functional differences between Pulv subregions [12, 18]. The dorsomedial portions include multimodal neurons preferentially connected to the AMG and to frontal areas [19]. Note, in fact, that reconstructed fibers reaching frontal areas passed through this Pulv division. Conversely, inferolateral Pulv portions are predominately visual and are bidirectionally connected with striate and extrastriate visual areas [18]. These latter Pulv subregions receive direct afferents from the SC and from the retina and are functionally homologous to the Pulv regions recently found to send efferents to the AMG and involved in the disynaptic SC-Pulv-AMG pathway in

nonhuman primates [12]. There was no significant difference in the Pulv-AMG connection strength between the LH (0.02 ± 0.008) and RH (0.031 ± 0.014) of controls [t(9) = 0.756, p = 0.469].

Patient G.Y.

In G.Y.'s (intact) RH, the fibers connecting the right Pulv and AMG extended to/from the same ipsilateral areas and were qualitatively similar to the fibers reconstructed in controls, including the presence of two subset of fibers to/from different Pulv divisions (Figure 2B). Quantitatively, the connection strength between right Pulv and AMG (0.021) was similar to that of controls, with no significant difference [t(9) = 0.72, p = 0.49]. In contrast, in the (damaged) LH, the fibers passing through the left Pulv and AMG continued to ipsilateral extrastriate areas V2/V3, temporal pole, SC, and brainstem. Therefore, fibers connecting left Pulv and AMG apparently did not extend to frontal areas but rather to posterior visual areas.
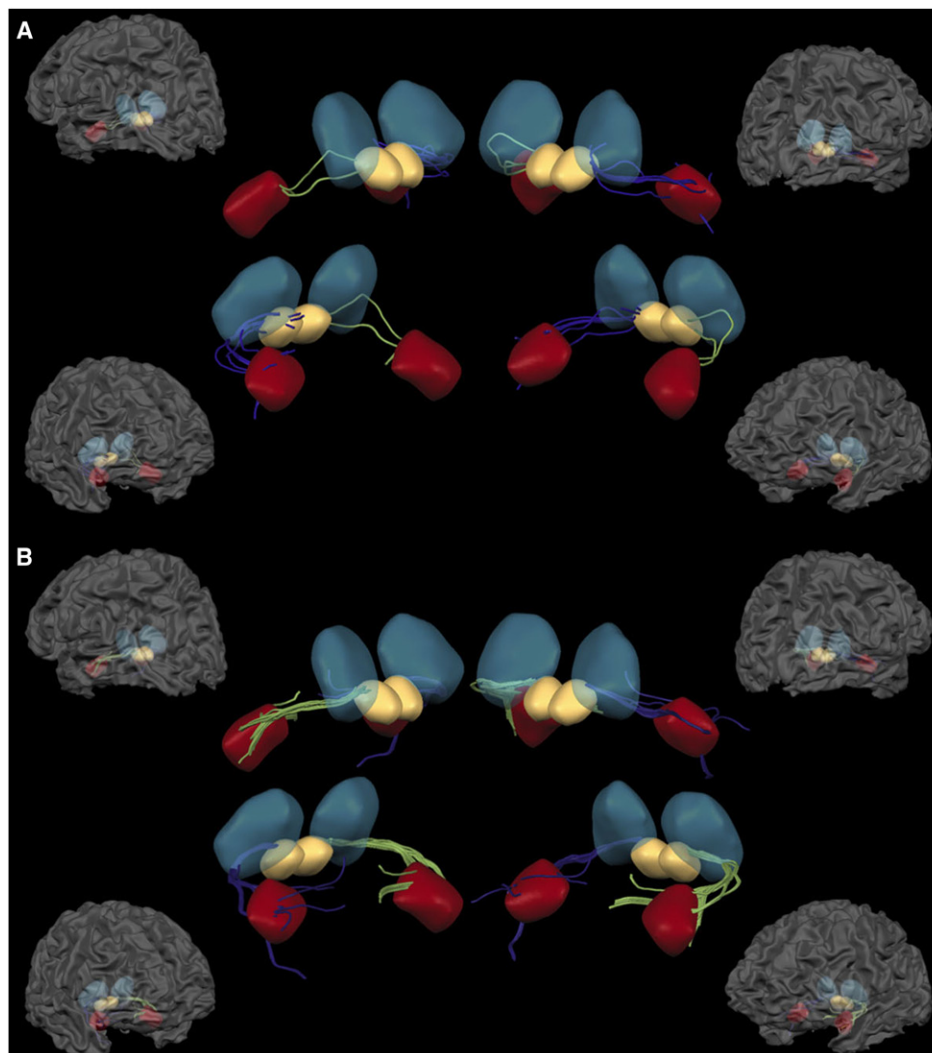
Figure 3. Reconstructed Fiber Tracts Constituting the Direct SC-Pulv-AMG Pathway

(A) Fiber tracts constituting the direct SC-Pulv-AMG pathway in the LH (green) and RH (blue) of one representative age-matched control subject.
(B) The same pathway in patient G.Y. Note that the Pulv is made transparent in order to display that the fibers run interruptedly between the SC and AMG passing through the inferolateral visual portions of the Pulv (see also Movie S1).

The connection between left Pulv and AMG of G.Y. (0.058) was almost 3-fold stronger (272%) than that found in his RH and in the LH of controls (287%), a difference that was highly significant [t(9) = 5.01, p < 0.001].

SC-Pulv-AMG Pathway
Controls
We were able to trace fibers that selectively and uninterruptedly connect the ipsilateral SC, Pulv, and AMG in both hemispheres of the controls (Figure 3A). Consistent with previous histological evidence in nonhuman primates, the fibers to/from the SC crossed the inferolateral visual portions of the Pulv before connecting with the AMG. It is, however, beyond the limits of DTI to assess whether these fibers make a synaptic relay in the visual Pulv. In both cases, the reconstructed fibers did not extend to/from any other cortical or subcortical structure, including the nonvisual subregions of the Pulv or extrastriate visual areas. There was no significant difference in the connection strength between LH (0.015 ± 0.009) and RH (0.25 ± 0.11) [t(9) = 2.147, p = 0.49].

Patient G.Y.
The same SC-Pulv-AMG pathway was reconstructed in LH and RH of G.Y. (Figure 3B). Also in this case, the fibers did not extend to/from other brain areas. Quantitative analysis showed that there was almost a 10-fold increase (995%) in the strength of the connection in the (damaged) LH (0.24) of G.Y. compared to that estimated in his (intact) RH (0.024), and almost a 16-fold increase (1571%) compared to the mean connection strength in the LH of controls. The connection strength in the SC-Pulv-AMG pathway of G.Y. differed significantly from that estimated in controls only in the (damaged) LH [t(9) = 23.85, p < 0.0001].

Fractional Anisotropy Analysis
For each hemisphere and pathway investigated, we independently extracted fractional anisotropy (FA) values from each voxel spatially located where the tractography algorithm reconstructed a fiber (Figure 4). FA values characterize the diffusion properties in each voxel [20], thereby providing a measure of anisotropy that is unaffected by the specific tractography
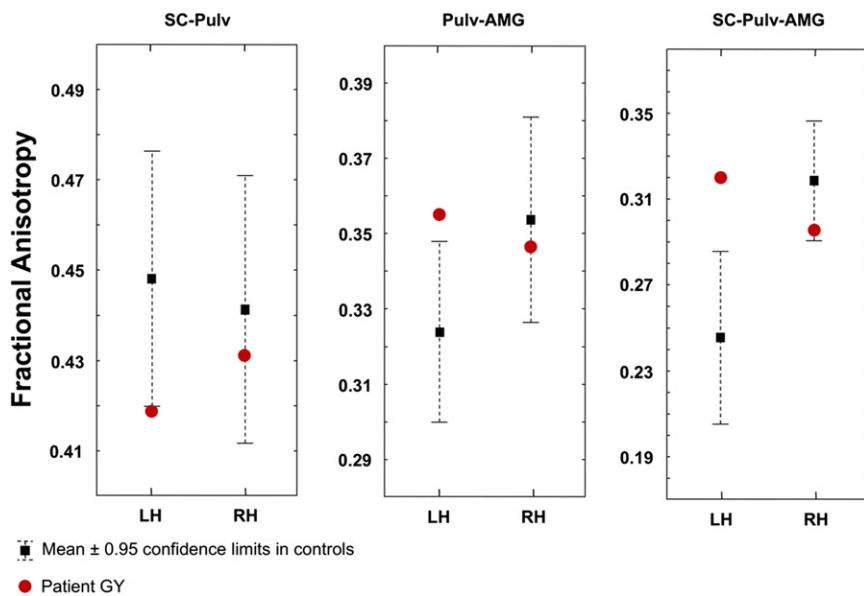
Figure 4. Fractional Anisotropy Values in the Controls and in Patient G.Y.

Mean fractional anisotropy values (±0.95 confidence limits) for each pathway and hemisphere in the ten age-matched controls and in patient G.Y.

patients [23] as well as in healthy subjects [24] showing that activation in the prefrontal cortex (in particular Brodmann area 46) is selectively associated to conscious stimulus perception.

The Pulv-AMG pathway in the (intact) RH of G.Y. was qualitatively and quantitatively comparable to the homologous pathway in the RH of controls. This shows that changes in connectivity as well as formation of interhemispheric tracts are not unspecific consequences of V1 damage, which instead affects selectively several pathways while leaving others substantially unchanged.

technique used. Results based on FA values paralleled those obtained on connection strength values. In fact, there was no significant difference between G.Y. and controls on FA values recorded in voxels along the SC-Pulv pathway in the RH [t(9) = 0.71, p = 0.5], whereas the difference was significant in the LH [t(9) = 2.31, p = 0.046]. In the Pulv-AMG pathway, there was a significant increase of FA in the (damaged) LH of G.Y. compared to controls [t(9) = 2.89, p = 0.018], but not in the (intact) RH [t(9) = 0.53, p = 0.61]. Finally, FA values in the SC-Pulv-AMG pathway were significantly higher in G.Y.'s (damaged) LH compared to controls [t(6) = 4.56, p = 0.004], but not in the (intact) RH [t(7) = 2.1, p = 0.07].

Discussion

In the present study, we characterized in vivo the anatomical connectivity between the SC, Pulv, and AMG and its changes following early loss of V1. Our results provide unequivocal evidence of qualitative and quantitative modifications along the pathways connecting these three structures. These changes consist in the strengthening of several fiber tracts already existing in the intact brain as well as in the formation of seemingly new tracts not otherwise present.

Fiber tracts connecting the SC and Pulv in the (intact) RH of G.Y. were of similar strength to those reconstructed in age-matched controls. However, the contralateral projections to/from posterior regions of the (damaged) LH were considerably more prominent than those found in control subjects. The homologous SC-Pulv pathway in the (damaged) LH of G.Y. was reduced in strength, failed to extend to frontal areas identified in controls and showed more connections to/from contralateral posterior areas in the RH. These findings are consistent with recent evidence in G.Y. and other patients with cortical blindness showing that V1 damage increases interhemispheric connections between homologous cortical areas as well as between subcortical and cortical visual structures in the opposite hemispheres with respect to the predominant ipsilateral connections found in controls [21, 22]. The reduced input to frontal areas in the damaged hemisphere is also remarkably consistent with prior functional results in cortically blind

Conversely, there was a strengthening of Pulv-AMG connections in the (damaged) LH of G.Y. compared to controls, and fiber tracts extended more posteriorly to visual areas than anteriorly to frontal regions.

Lastly, we traced the direct SC-Pulv-AMG pathway, therefore extending to the living human brain anatomical findings hitherto described only with the use of histological methods in nonhuman primates [12]. Nevertheless, independent confirmation with tracer methods in human postmortem studies is needed to consider this evidence to be conclusive. This pathway displays specific anatomical characteristics that cannot be considered the simple summation of the connectivity properties found individually in the SC-Pulv and in the Pulv-AMG pathways. In fact, when the analysis was constrained to the fibers selectively connecting these three structures, only a subset of fiber bundles was reconstructed among those found to connect SC-Pulv and Pulv-AMG. This subset of fibers passed through the visual subregion of the Pulv and did not extend to/from other cortical or subcortical structures. Moreover, the same pathway was also reconstructed in both hemispheres of G.Y., but the strength of the connection was higher in his (damaged) LH compared to controls, therefore strongly suggesting that it conveys V1-independent visual information.

The existence of continuous fiber tracts connecting the SC, Pulv, and AMG does not necessarily imply that these pathways are functionally relevant in underlying residual processing of emotions in the absence of V1 and of visual awareness. Moreover, there is a multitude of V1-independent pathways underlying different aspects of nonconscious perception [25], and there are many alternative anatomical routes possibly relaying visual information to the AMG from extrastriate visual cortex [14]. These alternative pathways presumably coexist with the subcortical SC-Pulv-AMG route and could contribute to the nonconscious perception of emotions [26]. However, it is straightforward to relate the anatomical results reported here to the functional evidence repeatedly showing activation of the SC, Pulv, and AMG when emotional stimuli are projected in the blind visual field of G.Y. [2, 5, 16]. Moreover, the same structures are also activated in neurologically intact subjects

during early stages of emotion processing [7–9] or when nonconscious perception of emotions is induced by experimental procedures such as visual masking [1, 3, 6, 27], flash suppression [28], or binocular rivalry [29] (see also [15] for a recent review). In particular, functional neuroimaging findings in G.Y. [2, 5] and healthy subjects [6, 30] have shown that nonconscious processing of emotional stimuli often results in the reduction or lack of cortical activity, especially in frontal areas, which is nevertheless normally present during conscious perception of the same stimuli. This is in keeping with the present anatomical data showing that the fiber tracts constituting the direct SC-Pulv-AMG pathway in both healthy controls and patient G.Y. do not continue to/from other cortical areas, in contrast to what was found for the SC-Pulv or Pulv-AMG pathways. Therefore, conscious and nonconscious perception of emotions seem to be mediated by neural systems that are partially segregated at the anatomical as well as functional level, and that undergo considerable neural plasticity and macroscopic anatomical reorganization following early destruction of V1.

Limitations of DTI

There are several methodological limitations to the conclusions that can be drawn from DTI results. First, it is not possible to establish the directionality of a pathway and to differentiate between anterograde, retrograde, or bidirectional connections between two or more structures. Our main hypothesis was based on feedforward connections from the SC to the AMG with a synaptic relay in the visual Pulv [12], but this possibility cannot find direct support in our data and remains speculative at present.

Second, DTI cannot support claims about whether a reconstructed fiber tract that passes through one or more gray matter structures is indicative of a monosynaptic or polysynaptic axonal pathway. In fact, DTI does not actually detect neurons or axons but only units of volumes and reconstructed fiber bundles, each of them containing thousands of neurons and axons. Again, we note that our results of uninterrupted streamlines connecting the SC with the AMG passing through the inferolateral visual portions of the Pulv are consistent with histological findings of a disynaptic pathway [12]. In fact, because of the spatial continuity between the (supposed) afferent fibers from SC to the inferolateral Pulv and the efferent fibers that (after the synaptic relay) should originate from the same inferolateral Pulv to reach AMG, the tractography was expected to find an uninterrupted fiber bundle, which is exactly what was observed.

A third limitation concerns the interpretation of the presence or absence of a given pathway and the risks of false positives. There is convincing evidence that in coherent white matter regions, the direction of diffusion corresponds to the principal axis of fiber direction [31, 32] and that tractography in such regions matches well with human postmortem data [33]. In regions of fiber crossing, or of degeneration, however, the relationship between DTI-reconstructed fiber bundles and the underlying axonal architecture is not yet fully understood. Therefore, our evidence about the existence of a direct SC-Pulv-AMG pathway or about connections between visual Pulv and AMG in the human brain requires independent confirmation with tracer methods in postmortem studies.

Nevertheless, we adopted several strategies to minimize the risk of false positives. One is that we used deterministic fiber tracking, which is less liable to false positives than probabilistic fiber tracking [17]. Moreover, errors and false positives in fiber

tracking increase with distance between the targeted regions [34], when fibers get closer to the cortex and/or to the cerebrospinal fluid (CSF) [35], and when fibers approach a lesion [21]. In the present case, we focused on relatively short fibers, located far from the cortex and from CSF and very distant from the lesion to V1. Moreover, for each pathway considered, we reversed seed and target regions, such that fibers were reconstructed in both directions. This procedure has proved to be a good strategy to detect possible tractography biases, especially false positives [21]. Lastly, our choice to follow the continuation of reconstructed fiber tracts beyond the targeted regions offered a valuable opportunity to assess, in a data-driven fashion, the reliability of the tractography algorithm and its consistency with tracts certainly known to exist from previous postmortem studies in humans. As summarized in Table S4, our results were in excellent agreement with previous studies and there were no false positives, as all reconstructed fiber bundles corresponded to existing axonal projections.

Because our tractography data remained highly consistent across subjects and hemispheres and all reconstructed fibers corresponded to existing axonal pathways, an interpretation of our novel findings in terms of false positives appears unlikely.

Experimental Procedures

Participants

Patient G.Y. is a well-documented male patient with right homonymous hemianopia and "blindsight." G.Y. was aged 53 at the time of testing and his visual system, including his residual ability to process emotions, has been studied extensively in previous reports using behavioral [36] and psychophysiological methods [37], as well as with neuroimaging techniques such as fMRI [38, 39], MEG [40], and DTI [21].

Ten age-matched healthy male controls with normal or corrected to normal vision and no previous history of neurological or psychiatric deficits participated in this study (see Table S1). Informed consent was obtained from all participants and the study was approved by the local Ethic Committee in accordance with the ethical standards laid down in the Declaration of Helsinki.

DTI Data Acquisition and Analysis

DTI characterizes the random microscopic motion (diffusion) properties of water molecules, which can be used to reconstruct white matter fiber bundles in the brain [41]. In fact, the diffusivity is anisotropic in large parts of the white matter, with the principal diffusion direction corresponding to the orientation of the major fiber tracts in each voxel [20]. Local (voxel-wise) orientation can then be followed through space to trace distant connections between brain areas [32].

Diffusion-weighted MRI data were acquired at Maastricht University, The Netherlands, on a 3T Siemens Allegra system (Siemens, Erlangen, Germany). In the same session, a T1-weighted anatomical image was acquired for registration and anatomical localization purposes. The three regions of interest (ROIs) (i.e., the SC, Pulv, and AMG) were defined anatomically and individually for each hemisphere and subject in T1-weighted structural images (see Supplemental Information, Figure S1, and Table S1).

Diffusion-weighted data were coregistered to the anatomical data, and the diffusion tensor was calculated in each voxel (2 mm^3) [41]. The ROIs were sampled with a dense grid of seed point (343 seeds/voxel) to start fiber tracking. The data were then exported to an in-house developed C/C++ tool for deterministic fiber tracking. Streamline fiber tracking used the local tensor as a projection operator [42] and was performed forward and backward between SC-Pulv, Pulv-AMG, and SC-PLV-AMG (i.e., the seed and target ROIs were reversed). A series of single sample t-tests were used for statistical comparisons of the mean connection strength in healthy controls with the connection strength in the corresponding pathway of G.Y., whereas a series of paired-sample t tests were used for statistical comparison of the mean connection strength in the same pathway between the LH and RH of controls. For details on experimental procedures and data analysis, see Supplemental Information.

Supplemental Information

Supplemental Information includes four figures, four tables, Supplemental Experimental Procedures, and one movie and can be found with this article online at doi:10.1016/j.cub.2012.06.006.

References

1. Liddell, B.J., Brown, K.J., Kemp, A.H., Barton, M.J., Das, P., Peduto, A., Gordon, E., and Williams, L.M. (2005). A direct brainstem-amygdala-cortical 'alarm' system for subliminal signals of fear. Neuroimage 24, 235–243.

2. Morris, J.S., DeGelder, B., Weiskrantz, L., and Dolan, R.J. (2001). Differential extrageniculostriate and amygdala responses to presentation of emotional faces in a cortically blind field. Brain 124, 1241–1252.

3. Morris, J.S., Ohman, A., and Dolan, R.J. (1999). A subcortical pathway to the right amygdala mediating "unseen" fear. Proc. Natl. Acad. Sci. USA 96, 1680–1685.

4. Pegna, A.J., Khateb, A., Lazeyras, F., and Seghier, M.L. (2005). Discriminating emotional faces without primary visual cortices involves the right amygdala. Nat. Neurosci. 8, 24–25.

5. Van den Stock, J., Tamietto, M., Sorger, B., Pichon, S., Grézes, J., and de Gelder, B. (2011). Cortico-subcortical visual, somatosensory, and motor activations for perceiving dynamic whole-body emotional expressions with and without striate cortex (V1). Proc. Natl. Acad. Sci. USA 108, 16188–16193.

6. Whalen, P.J., Rauch, S.L., Etcoff, N.L., McInerney, S.C., Lee, M.B., and Jenike, M.A. (1998). Masked presentations of emotional facial expressions modulate amygdala activity without explicit knowledge. J. Neurosci. 18, 411–418.

7. Garrido, M.I., Barnes, G.R., Sahani, M., and Dolan, R.J. (2012). Functional evidence for a dual route to amygdala. Curr. Biol. 22, 129–134.

8. Luo, Q., Holroyd, T., Jones, M., Hendler, T., and Blair, J. (2007). Neural dynamics for facial threat processing as revealed by gamma band synchronization using MEG. Neuroimage 34, 839–847.

9. Vuilleumier, P., Armony, J.L., Driver, J., and Dolan, R.J. (2003). Distinct spatial frequency sensitivities for processing faces and emotional expressions. Nat. Neurosci. 6, 624–631.

10. Doron, N.N., and Ledoux, J.E. (1999). Organization of projections to the lateral amygdala from auditory and visual areas of the thalamus in the rat. J. Comp. Neurol. 412, 383–409.

11. LeDoux, J.E. (1996). The Emotional Brain (New York: Simon & Schuster).

12. Day-Brown, J.D., Wei, H., Chomsung, R.D., Petry, H.M., and Bickford, M.E. (2010). Pulvinar projections to the striatum and amygdala in the tree shrew. Front Neuroanat 4, 143.

13. Cowey, A. (2010). The blindsight saga. Exp. Brain Res. 200, 3–24.

14. Pessoa, L., and Adolphs, R. (2011). Emotion processing and the amygdala: from a 'low road' to 'many roads' of evaluating biological significance. Nat. Rev. Neurosci. 11, 773–783.

15. Tamietto, M., and de Gelder, B. (2010). Neural bases of the non-conscious perception of emotional signals. Nat. Rev. Neurosci. 11, 697–709.

16. de Gelder, B., Morris, J.S., and Dolan, R.J. (2005). Unconscious fear influences emotional awareness of faces and voices. Proc. Natl. Acad. Sci. USA 102, 18682–18687.

17. Yo, T.S., Anwander, A., Descoteaux, M., Fillard, P., Poupon, C., and Knösche, T.R. (2009). Quantifying brain connectivity: a comparative tractography study. Med Image Comput Comput Assist Interv 12, 886–893.

18. Grieve, K.L., Acuña, C., and Cudeiro, J. (2000). The primate pulvinar nuclei: vision and action. Trends Neurosci. 23, 35–39.

19. Jones, E.G., and Burton, H. (1976). A projection from the medial pulvinar to the amygdala in primates. Brain Res. 104, 142–147.

20. Mori, S., and van Zijl, P.C. (2002). Fiber tracking: principles and strategies - a technical review. NMR Biomed. 15, 468–480.

21. Bridge, H., Thomas, O., Jbabdi, S., and Cowey, A. (2008). Changes in connectivity after visual cortical brain damage underlie altered visual function. Brain 131, 1433–1444.

22. Leh, S.E., Johansen-Berg, H., and Ptito, A. (2006). Unconscious vision: new insights into the neuronal correlate of blindsight using diffusion tractography. Brain 129, 1822–1832.

23. Sahraie, A., Weiskrantz, L., Barbur, J.L., Simmons, A., Williams, S.C., and Brammer, M.J. (1997). Pattern of neuronal activity associated with conscious and unconscious processing of visual signals. Proc. Natl. Acad. Sci. USA 94, 9406–9411.

24. Lau, H.C., and Passingham, R.E. (2006). Relative blindsight in normal observers and the neural correlate of visual consciousness. Proc. Natl. Acad. Sci. USA 103, 18763–18768.

25. Schmid, M.C., Mrowka, S.W., Turchi, J., Saunders, R.C., Wilke, M., Peters, A.J., Ye, F.Q., and Leopold, D.A. (2010). Blindsight depends on the lateral geniculate nucleus. Nature 466, 373–377.

26. de Gelder, B., van Honk, J., and Tamietto, M. (2011). Emotion in the brain: of low roads, high roads and roads less travelled. Nat. Rev. Neurosci. 12, 425.

27. Whalen, P.J., Kagan, J., Cook, R.G., Davis, F.C., Kim, H., Polis, S., McLaren, D.G., Somerville, L.H., McLean, A.A., Maxwell, J.S., and Johnstone, T. (2004). Human amygdala responsivity to masked fearful eye whites. Science 306, 2061.

28. Vizueta, N., Patrick, C.J., Jiang, Y., Thomas, K.M., and He, S. (2011). Dispositional fear, negative affectivity, and neuroimaging response to visually suppressed emotional faces. Neuroimage 59, 761–771.

29. Williams, M.A., Morris, A.P., McGlone, F., Abbott, D.F., and Mattingley, J.B. (2004). Amygdala responses to fearful and happy facial expressions under conditions of binocular suppression. J. Neurosci. 24, 2898–2904.

30. Anderson, A.K., Christoff, K., Panitz, D., De Rosa, E., and Gabrieli, J.D. (2003). Neural correlates of the automatic processing of threat facial signals. J. Neurosci. 23, 5627–5633.

31. Lin, C.P., Tseng, W.Y., Cheng, H.C., and Chen, J.H. (2001). Validation of diffusion tensor magnetic resonance axonal fiber imaging with registered manganese-enhanced optic tracts. Neuroimage 14, 1035–1047.

32. Thiebaut de Schotten, M., Ffytche, D.H., Bizzi, A., Dell'Acqua, F., Allin, M., Walshe, M., Murray, R., Williams, S.C., Murphy, D.G., and Catani, M. (2011). Atlasing location, asymmetry and inter-subject variability of white matter tracts in the human brain with MR diffusion tractography. Neuroimage 54, 49–59.

33. Stieltjes, B., Kaufmann, W.E., van Zijl, P.C., Fredericksen, K., Pearlson, G.D., Solaiyappan, M., and Mori, S. (2001). Diffusion tensor imaging and axonal tracking in the human brainstem. Neuroimage 14, 723–735.

34. Lazar, M. (2010). Mapping brain anatomical connectivity using white matter tractography. NMR Biomed. 23, 821–835.

35. Jones, D.K. (2008). Studying connections in the living human brain with diffusion MRI. Cortex 44, 936–952.

36. de Gelder, B., Vroomen, J., Pourtois, G., and Weiskrantz, L. (1999). Non-conscious recognition of affect in the absence of striate cortex. Neuroreport 10, 3759–3763.

37. Tamietto, M., Castelli, L., Vighetti, S., Perozzo, P., Geminiani, G., Weiskrantz, L., and de Gelder, B. (2009). Unseen facial and bodily expressions trigger fast emotional reactions. Proc. Natl. Acad. Sci. USA 106, 17661–17666.

38. Goebel, R., Muckli, L., Zanella, F.E., Singer, W., and Stoerig, P. (2001). Sustained extrastriate cortical activation without visual awareness revealed by fMRI studies of hemianopic patients. Vision Res. 41, 1459–1474.

39. Tamietto, M., Cauda, F., Corazzini, L.L., Savazzi, S., Marzi, C.A., Goebel, R., Weiskrantz, L., and de Gelder, B. (2010). Collicular vision guides nonconscious behavior. J. Cogn. Neurosci. 22, 888–902.

40. Holliday, I.E., Anderson, S.J., and Harding, G.F. (1997). Magnetoencephalographic evidence for non-geniculostriate visual input to human cortical area V5. Neuropsychologia 35, 1139–1146.

41. Basser, P.J., Mattiello, J., and LeBihan, D. (1994). MR diffusion tensor spectroscopy and imaging. Biophys. J. 66, 259–267.

42. Westin, C.F., Maier, S.E., Mamata, H., Nabavi, A., Jolesz, F.A., and Kikinis, R. (2002). Processing and visualization for diffusion tensor MRI. Med. Image Anal. 6, 93–108.